Stereo Vision-based Visual Tracking using 3D Feature Clustering for Robust Vehicle Tracking

Young-Chul Lim and Minsung Kang
*Division of Advanced Industrial Science and Technology, Daegu Gyeongbuk Institute of Science & Technology, Room 511,
5th floor, 3rd Research Center, 333, Techno Jungang Daero, Hyeonpung-myeon, Dalseong-gun,
Daegu, 711-873, Republic of Korea*

Keywords: Object Tracking, Feature Tracking, Feature Clustering, Stereo Vision.

Abstract: In order to detect vehicles on the road reliably, a vehicle detector and tracker should be integrated to work in unison. In real applications, some of the ROIs generated from a vehicle detector are often ill-fitting due to imperfect detector outputs. The ill-fitting ROIs make it difficult for tracker to estimate a target vehicle correctly due to outliers. In this paper, we propose a stereo-based visual tracking method using a 3D feature clustering scheme to overcome this problem. Our method selects reliable features using feature matching and a 3D feature clustering method and estimates an accurate transform model using a modified RANSAC algorithm. Our experimental results demonstrate that the proposed method offers better performance compared with previous feature-based tracking methods.

1 INTRODUCTION

Robust object detection and tracking are very important for driving assistance systems and safe driving. Recognizing a vehicle's surroundings can reduce the number of traffic accidents caused by careless driving. In the field of intelligent vehicles, many researchers have worked on detecting and tracking various objects, such as vehicles, pedestrians, and traffic signs. Many researchers have made their best efforts to improve the reliability of object detection methods (Sivaraman and Trivedi, 2013). However, no state-of-the-art detection method can detect all objects on the road without false detections. In order to enhance the detection performance, the best way is to integrate detection and tracking algorithms. Even if the detector misses a target object in the current frame, visual tracking can localize the target object using the motion information in the previous frames.

In visual tracking methods, the traditional and fundamental approach is template matching, but its limitation is a high computational cost due to its repetitive comparison process. A mean shift (MS) is a simple iterative nonparametric density analysis that is essentially a gradient ascent algorithm with an adaptive step size (Cheng, 1995). The kernel-based tracking method uses a spatially smoothing similarity function with a Bhattacharyya coefficient and a gradient optimization method with mean shift for target localization (Comaniciu et al., 2008). A combined method with an adaptive Kalman filter (KF) and a mean shift was proposed to localize the target position accurately when the object undergoes a large degree of displacement or occlusion (Xiaohe et al., 2010). Particle filter-based tracking approaches compare appearance similarities such as color, edge, and texture within candidate regions and select the most likely ROI (Adam et al., 2010).

Feature-based tracking methods estimate the state of a target while calculating the displacement of distinctive features and estimating a transform model using the random sample consensus (RANSAC) algorithm (Rodrigo et al., 2010). The Kanade-Lucas-Tomasi (KLT) method (Jianbo and Tomasi, 1994) employs an iterative optimization scheme that finds distinct features in the current frame and then attempts to find a correspondence in the next frame. In order to handle any large displacement due to abrupt motion, a pyramidal KLT method estimates the motion vector by computing the iterative optical flow (Bouguet, 2010). A modified KLT method uses conventional KLT in conjunction with a symmetric-based tracker for tracking bilaterally symmetric planar objects such as pedestrians and vehicles on the road

Lim Y. and Kang M..
Stereo Vision-based Visual Tracking using 3D Feature Clustering for Robust Vehicle Tracking.
DOI: 10.5220/0005147807880793
In *Proceedings of the 11th International Conference on Informatics in Control, Automation and Robotics* (IVC&ITS-2014), pages 788-793
ISBN: 978-989-758-040-6

(Schreiber, 2009). Feature based-tracking methods deteriorate the matching accuracy due to intensity ambiguities in pixels, and some researchers have introduced a combined method which utilizes the advantages of appearance and feature matching (Khan and Gu, 2010).

Visual tracking aims to find the movement of an object onto a current image from a previous image. Recent feature-based visual tracking methods have focused on enhancing robustness against very poor conditions, as characterized by abrupt motions, appearance and rotation changes, illumination changes, and partial occlusion, for instance. The way to evaluate these approaches is to determine how well the tracker estimates the ROI after the first image is manually annotated by a well-fitting ROI. In real applications, the ROI is generally generated by a detector, and the ROI is often ill-fitting due to noisy detector outputs. There may be many outliers in an ill-fitting ROI, which cause a track drifting problem. In order to track an ill-fitting target object robustly, it is necessary to remove the outliers. In this paper, a feature-based visual tracking method using 3D feature clustering is proposed and shown to be robust against an ill-fitting ROI.

The rest of our paper is organized as follows. In Section 2, we give an overview of our feature-based tracking method. Section 3 explains the 3D feature clustering scheme using position and motion displacement in global coordinates. Experimental results and analyses of real-world image sequences are presented in Section 4. Finally, Section 5 concludes this paper with suggestions for future works.

2 OVERVIEW OF OUR VISUAL TRACKING METHOD

Our feature-based visual tracking method is proposed to be robust against an ill-fitting ROI. The method consists of pre-processing, feature extraction, feature tracking, feature matching, 3D feature clustering, and ROI estimation, as shown in Figure 1. The feature matching and 3D feature clustering steps are used to select reliable inlier features.

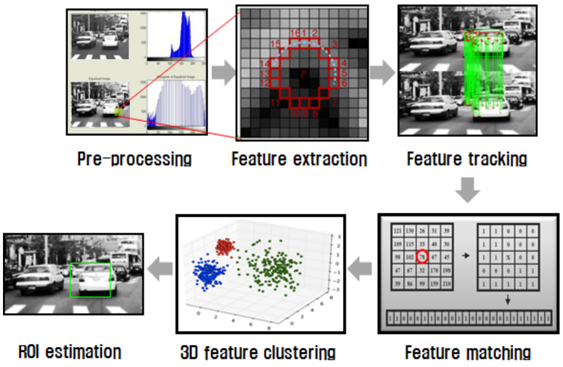

Figure 1: Architecture of the proposed feature tracking method.

In real road environments, the illumination condition is very poor. Pre-processing methods such as Gaussian smoothing and histogram equalization are very efficient to ensure robustness against a poor illumination condition. A features from accelerated segment test (FAST) detector (Rosten et al., 2010) is used to extract distinctive features due to its good speed and high level of accuracy. The FAST detector determines a point as a distinctive feature if *n* contiguous pixels exist in the circle of the point. The *n* pixels should all be brighter or darker than the intensity of the point. Each of the 16 surrounding pixels has one of three states which are represented by darker (d), brighter (b), and similar (s) pixels. In the feature tracking module, the KLT tracker localizes the correspondences of features extracted from the previous image. Erroneous corresponding feature pairs are removed by a feature matching method which utilizes binary feature matching. The census transform method (Zabih and Woodfill, 1994) and the Hamming distance are used to measure the similarity between the feature pairs which are estimated by the feature tracker. Census transform converts the pixel intensity to a binary pattern using the relative order of the local intensity. The similarity between binary patterns of the feature pairs are measured by the Hamming distance. This matching method is much more robust than the normalized cross-correlation (NCC) matching method near object boundaries (Zabih and Woodfill, 1994). Many features extracted from the FAST detector exist in the object boundaries. The feature matching algorithm is executed in the intensity image to remove incorrectly estimated feature pairs.

$$\begin{cases} if\left[D_H\left(T_C(f_{t-1}^{i}), T_C(f_t^{\sim i})\right) < \gamma\right], selected \\ else \qquad\qquad\qquad\qquad\qquad\quad , discarded \end{cases} \tag{1}$$

where $T_c(x)$ denotes the census transform function of feature x, and $D_H(a,b)$ indicates the Hamming distance between the a and b vectors. f_{t-1}^{i} and $f_t^{\sim i}$ denote the i^{th} feature in the previous frame and the paring feature in the current frame, respectively. γ is a fixed threshold value for selecting the features. In order to find outlier features, the 3D feature clustering module selects features corresponding to only the target object among selected features. The

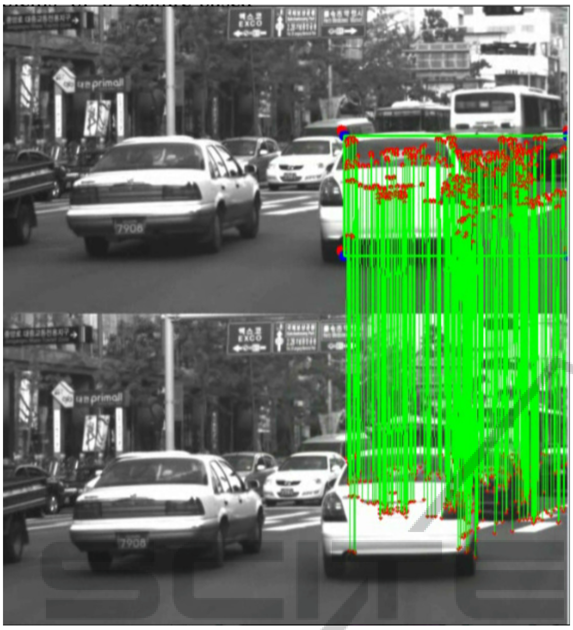

Figure 2: Outliers in an ill-fitting ROI.

mean and covariance of the features in terms of the global position and motion are iteratively updated by the Mahalanobis distance. The feature clustering step is finished when the mean of the feature position converge. The clustering features are used to estimate a transform model parameter. An affine transform is used for motion estimation of the target object in this work. Finally, the current ROI is estimated by the transform model and the previous ROI position.

3 3D FEATURE CLUSTERING

One of the difficult problems with feature-based visual tracking involves selecting the features corresponding to the target object. When a target object is estimated by an ill-fitting ROI from an object detector, there may be many outliers that correspond to background or other objects in the ROI, as shown in Figure 2. Consequently, the outliers make it difficult to estimate the transform model parameters accurately. The 3D feature clustering method tackles this problem while minimizing the number of these outliers. The features are clustered in a 3D global position and motion spaces using an iterative scheme. In this clustering method, the features are projected onto the 3D global coordinate using an inverse perspective mapping (IPM) model (Lim et al, 2010), where P_i^g denotes the 3D global position of the i^{th} feature. X_g, Y_g, and Z_g are feature positions on the global coordinates. x_{dl} and x_{dr} are horizontal positions on the left and right image coordinates. y_d indicates the vertical position in both image coordinates. d is the integer disparity of the feature. α and b are the focal distance expressed in units of pixels and a baseline that denotes the distance between the stereo cameras, respectively. h and θ denote the height of the cameras above the ground and the angle between the Z direction and the optical axis of the cameras, respectively. The Mahalanobis distance (d_m) is used for clustering the features in the 3D global coordinates.

$$P_i^g = \begin{bmatrix} X_g \\ Y_g \\ Z_g \end{bmatrix} = \begin{bmatrix} \frac{(x_{dl}+x_{dr})\left((Y_g+h)sin\theta+Z_g cos\theta\right)}{2\alpha} \\ \frac{by_d cos\theta+\alpha bsin\theta-dh}{d} \\ \frac{b(\alpha cos\theta-y_d sin\theta)}{d} \end{bmatrix}, \qquad (2)$$

$$\begin{cases} if\left(d_m(P_i^g) > T_p\right), & selected, \\ else & , \; discarded, \end{cases} \qquad (3)$$
$$d_m(P_i^g) = \left(P_i^g - P_m^g\right)^T \delta_p^{-1}\left(P_i^g - P_m^g\right),$$

where P_m^g and δ_p denote the mean and covariance of the features in the 3D global position. T_p is a threshold value for discarding the outliers. The displacement of selected features is calculated for 3D global motion clustering in the global coordinates.

$$\begin{cases} if\left(d_m(M_i) > T_M\right), & selected, \\ else & , \; discarded, \end{cases} \qquad (4)$$
$$d_m(M_i) = (M_i - M_m)^T \delta_M^{-1}(M_i - M_m),$$

where M_i indicates the motion vector of the i^{th} feature in the global coordinate, M_m and δ_M are the mean and covariance of the motion vectors in the global coordinate. T_M is a threshold value related to the motion vector. The mean and covariance of features are updated by the clustered features at each iterative epoch. The features are iteratively selected and rejected until the mean of the motion vector converges to the global coordinate. The finally selected features are used to estimate an optimal transform matrix $\hat{T}_t$ with the modified RANSAC method.

Table 1: Summary of the test datasets.

	# of frame	characteristics
Scene 1	101	Size change
Scene 2	177	Poor illumination condition
Scene 3	100	Partial occlusion on a rainy day
Scene 4	200	Pose change in a cluttered environment

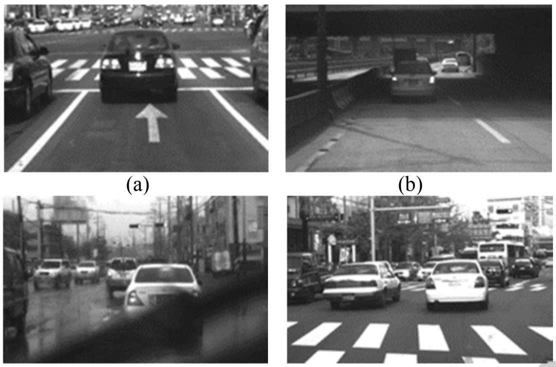
(a) (b)
(b) (d)

Figure 3: Test datasets for feature-based visual tracking. (a) Size change, (b) Illumination change, (c) Partial occlusion on a rainy day, (d) Pose change in a cluttered environment.

Table 2: Processing time (ms) of visual trackers.

	KLT	2D-SFVT	SURF	3D-SFVT
Scene 1	7.5	**7.3**	216.4	7.8
Scene 2	7.7	7.4	122.4	**7.2**
Scene 3	7.0	10.2	216.5	**6.5**
Scene 4	8.3	7.8	204.5	**6.9**

$$\hat{T}_t = \underset{T_t}{\operatorname{argmax}} \sum_{k=1}^{P} f_{MR}\left(T_t f_k^{t-1}, f_k^t\right), \qquad (5)$$

$$f_{MR}\left(\hat{f}_k, f_k\right) = e^{-\lambda_m \sqrt{\left(\hat{f}_k - f_k\right)^T \left(\hat{f}_k - f_k\right)}}$$

where P is the number of selected features, f_k^t is the k^{th} feature position in t frame, and λ_m has a constant value. The current ROI is estimated by the transform matrix $\hat{T}_t$ and the previous ROI.

4 EXPERIMENTAL RESULTS

Our feature-based visual tracking method was implemented with Visual C++ 9.0 and the OPENCV 2.2 library. Four test datasets were used for a quantitative evaluation and a qualitative analysis. They were captured from real road environments, as shown in Figure 3.

In Scene 1, the vehicle size grows steadily in the image while a distant vehicle is gradually approaching. In Scene 2, a target vehicle passes through a tunnel. An abrupt illumination change occurs when entering and exiting the tunnel. The test dataset contains a very dark lighting condition when the vehicle passes in the tunnel. In Scene 3, the test dataset was captured on a rainy day. The target vehicle was often occluded by the windshield wiper, and the target vehicle contains noisy regions due to raindrops. In Scene 4, the pose of the target vehicle changes in a road environment with heavy traffic, and many outliers exists in the ROI. A summary of test scenes is described in Table 1.

The target vehicle is manually annotated in the first frame, after which the trackers estimate the ROI of the target vehicle from the next frame. The annotated ROIs are ill-fitting while shifting the ROIs to the left and right to verify robustness against an ill-fitting ROI. The performances of the KLT tracker (Jianbo and Tomasi, 1994), SURF tracker (Bay et al., 2010), 2D selected-feature-based visual tracker (2D-SFVT) (Lim et al., 2010), and 3D selected feature-based tracker (3D-SFVT) are measured by the overlap ratio between ground truth regions and estimated regions.

As shown in Figure 4, the experimental results show that all trackers can estimate the ROIs well without errors when the ROI is initially well-fitting. However, most vehicle detectors often provide an inaccurate ROI. When the ROI is ill-fitting, previous tracking methods often provide poor tracking performance.

The tracking performances of all of the methods are similar in Scene 1. The 2D-SFVT method provides slightly better tracking performance when the ROI is well-fitting. In experimental results for Scene 2, the 3D-SFVT method provides the best tracking performance, especially when the ROIs are ill-fitting. In Scene 2, the pre-processing methods of a Gaussian smoothing filter and histogram equalization make the trackers robust against the poor illumination condition in the tunnel, as shown in Figure 5. Similar performances for all the trackers resulted for Scene 3. Although there are many feature matching errors occur due to occlusion and noisy pixel intensity in Scene 3, a modified RANSAC algorithm can estimate the correct transform matrix using only part of the selected features. When the ROI is ill-fitting in Scene 4, previous tracking methods generate track-drifting problems due to outliers. However, the 3D-SFVT method removes the outliers using feature matching and the 3D clustering method, and reliable tracking results can be achieved (Figure 6). In the test of the SURF tracker in Scene 4, track drifting problems occur, but the ROIs are fortunately readjusted to the target vehicle due to the field of view (FOV) of the camera. Table 2 shows the processing time of each visual tracker. The processing time of the SURF tracker is high, and the other visual trackers achieve similar runtimes.

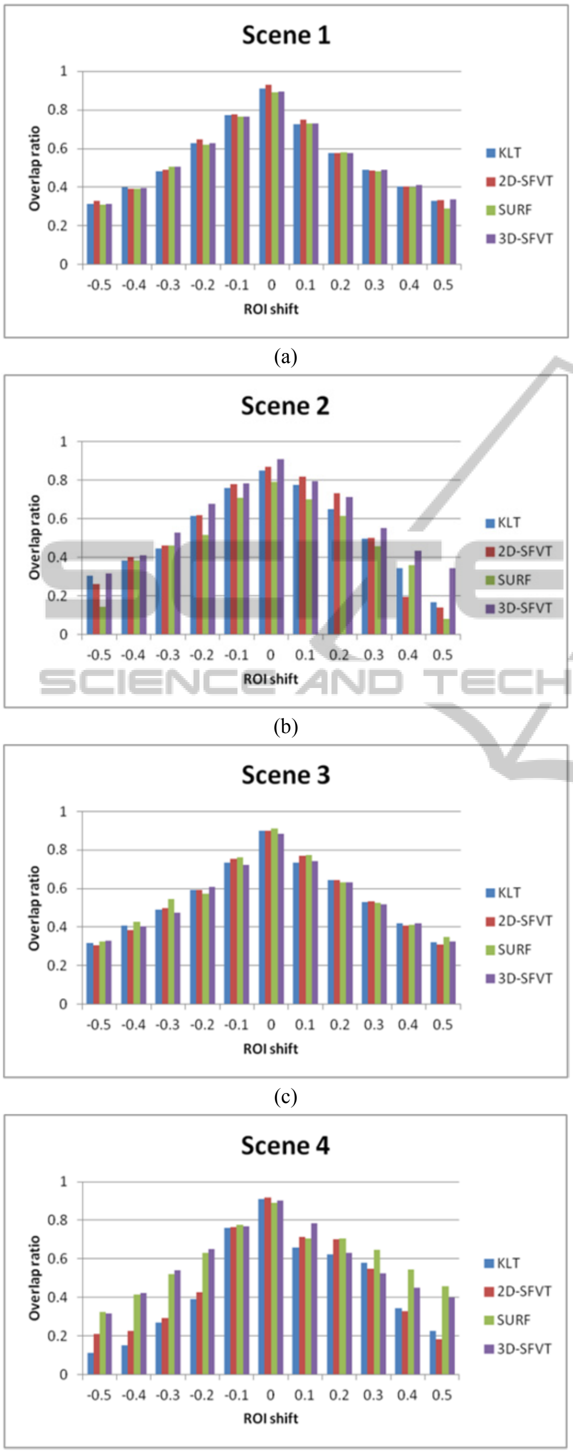

(a)

(b)

(c)

(d)

Figure 4: Experiment results of feature-based visual trackers. The ROI shift indicates that the ROI moves to the left (negative) and right (positive) directions, and the value denotes the shift proportion with regard to the width of ROI. (a) Scene 1, (b) Scene 2, (c) Scene 3, and (d) Scene 4.

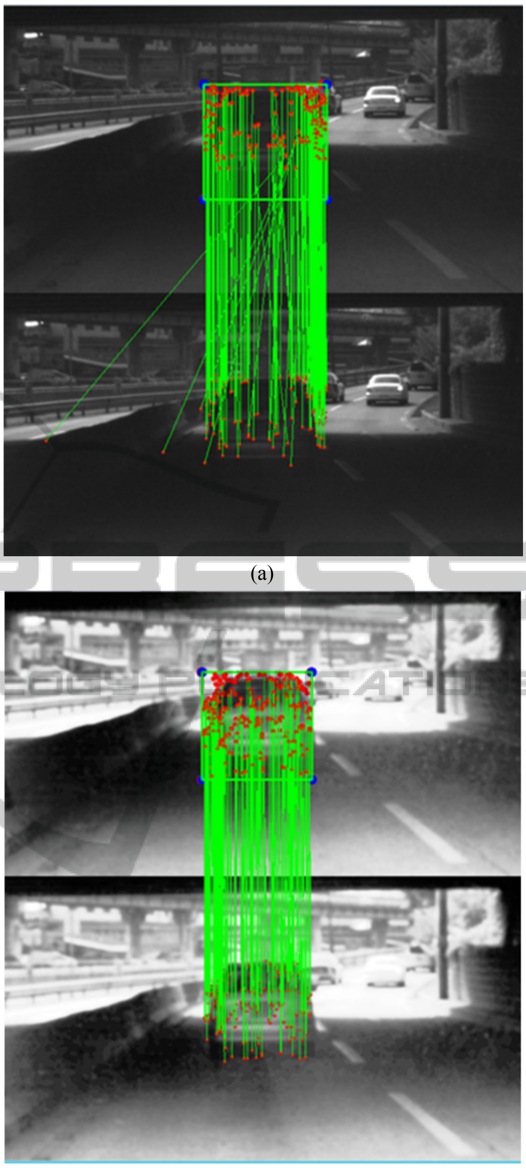

(a)

(b)

Figure 5: Feature matching results in Scene 2. (a) before pre-processing, and (b) after pre- processing.

5 CONCLUSIONS

In this paper, we proposed a stereo-based visual tracking method using 3D feature clustering. The features are projected onto a 3D global coordinate and reliable feature pairs are selected by feature matching and iterative 3D clustering schemes.

Model parameters and the ROI are estimated using the selected features and a modified RANSAC algorithm. The experimental results demonstrate that our method outperforms previous methods in the

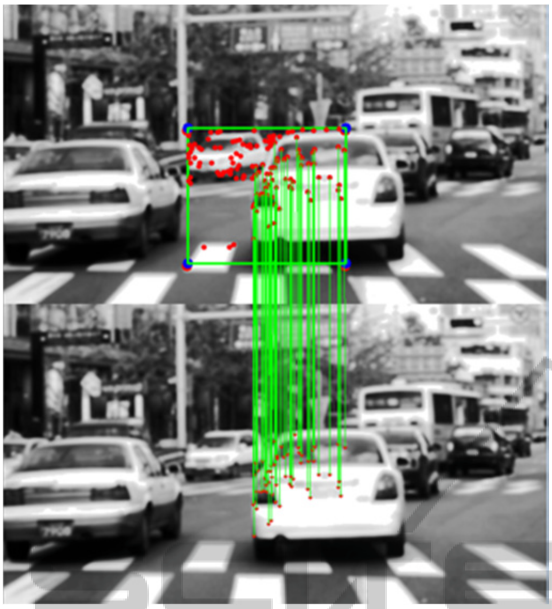

Figure 6: Feature matching results when the ROI shift is -0.4 in Scene 4.

presence of an ill-fitting ROI with reasonable processing times. In the future, we will combine the proposed tracker with a vehicle detector to enhance its vehicle detection performance.

ACKNOWLEDGEMENTS

This work was supported by the DGIST R&D Program of the Ministry of Science, ICT, and Future Planning of Korea.

REFERENCES

Adam, A., Rivlin, E., and Shimshoni, I., 2006. Robust fragments-based tracking using the integral histogram. Proceedings of IEEE Conference Computer Vision and Pattern Recognition, pp. 798-805.

Bay, H., Ess, A., Tuytelaars, T., and Gool, L. V., 2008. SURF: Speeded Up Robust Features. Computer Vision and Image Understanding, Vol. 110, no. 3, pp. 346-359.

Bouguet, J. -Y., 2010. Pyramidal implementation of the Lucas-Kanade feature tracker. http://robots.stanford.edu/cs223b04/algo_tracking.pdf.

Cheng, Y., 1995. Mean shift, mode seeking, and clustering. *IEEE Transactions on Pattern Analysis and Machine Intelligence*. Vol. 17, no. 8, pp. 790-799.

Comaniciu, D., Ramesh, V., and Meer, P., 2003. Kernel-based object tracking. IEEE Transactions on Pattern Analysis and Machine Intelligence. Vol. 25, no. 5, pp. 564-577.

Jianbo, S. and Tomasi, C., 1994. Good features to track. Proceedings of IEEE Conference Computer Vision and Pattern Recognition, pp. 593-600.

Khan, Z. H. and Gu, I. Y. -H., 2010. Joint feature correspondences and appearance similarity for robust visual object tracking. IEEE Transactions on Information Forensics and Security, Vol. 5, no. 3, pp. 591-606.

Lim, Y. -C., Lee, M., Lee, C. -H., Kwon, S., and Lee, J. -H., 2010. Improvement of stereo vision-based position and velocity estimation and tracking using a stripe-based disparity estimation and inverse perspective map-based extended Kalman filter. Optics and Lasers in Engineering, Vol. 48, no. 9, pp. 859-868.

Lim, Y. -C., Lee, M., Lee, C. -H., Kwon, S., and Lee, J.-H., 2011. Integrated position and motion tracking method for online multi-vehicle tracking-by-detection. Optical Engineering, Vol. 50, no. 7, 077203.

Rodrigo, R., Zouqi, M., Zhenhe, C., and Samarabandu, J., 2009. Robust and efficient feature tracking for indoor navigation. IEEE Transactions on Systems, Man, and Cybernetics, Part B: Cybernetics, Vol. 39, no. 3, pp. 658-671.

Rosten, E., Porter, R., and Drummond, T., 2010. Faster and better: a machine learning approach to corner detection. IEEE Transactions on Pattern Analysis and Machine Intelligence, Vol. 32, no. 1, pp. 105-119.

Schreiber, D., 2009. Incorporating symmetry into the Lucas-Kanade framework. Pattern Recognition Letters, Vol. 30, no. 7, pp. 690-698.

Sivaraman, S. and Trivedi, M.M., 2013. A Review of Recent Developments in Vision-Based Vehicle Detection. Proceedings of IEEE Intelligent Vehicle Symposium, pp. 310-315.

Xiaohe, L., Taiyi, Z. Xiaodong, S. and Jiancheng, S., 2010. Object tracking using an adaptive Kalman filter combined with mean shift. Optical Engineering Letters, Vol. 49, no. 2, 020503.

Zabih, R. and Woodfill, J., 1994. Non-parametric local transforms for computing visual correspondence. Proceedings of European Conference on Computer Vision, Vol. 2, pp. 151-158.